

Determination of Planck's constant using the photoelectric effect

ANDREW D. MILLER

Imperial College, London

adm114@ic.ac.uk | CID: 00929697

Laboratory Partner: Ian M. Yeung

December 3, 2016

Abstract

Utilising the properties of certain alkali metals and the particle-like properties of light, the photoelectric effect can be used to estimate the value of the fundamental constant h . A high pressure mercury lamp was directed onto a photocell through a series of lenses and spectral filters, and a small photocurrent was observed at specific frequencies. Applying a range of opposing voltages to the photocell caused the photocurrent to drop to zero, and plotting these voltages against the corresponding frequencies meant Planck's constant could be evaluated. Using three different methods of determine h , an average value of $(6.17 \pm 0.68) \times 10^{-34} \text{Js}$ was calculated.

I. INTRODUCTION

THE photoelectric effect is one of the most investigated phenomena in modern-day science, and since its discovery by Heinrich Hertz in 1887 [Hertz, 1887] and formal explanation by Albert Einstein in 1905 [Einstein, 1905], it has been shown to have a very broad range of consequences across many different areas of research. The photoelectric effect also has many applications, including use in automatic door light sensors, photomultipliers for detecting light, and even night vision goggles, and one of its major uses in physics research is the determination of Planck's constant, which has a value of $6.626070040(81) \times 10^{-34} \text{Js}$ [1]. One of the biggest repercussions of Einstein's solution was the proposal of the dual wave-particle nature of light, which in turn led to the foundation of much of quantum mechanics. According to classical wave theory, the energy of the photon is proportional to the intensity of the beam alone. This paper aims to prove that it is the quantum model of light that holds for this experiment, and also when a specific voltage is applied across a photodiode irradiated by photons such that the photoelectron flow is reduced to near zero, the constant of proportionality of this voltage with frequency is Planck's constant.

II. THEORY

From Einstein's theory of quantised light, the energy of photons from a source depends on both the photons'

frequency (ν) and the fundamental constant h (see Equation 1).

$$E = h\nu \quad (1)$$

It is also known that for all metals, there is a minimum binding energy for electrons in the material that is called the work function (ϕ), usually quoted in electron volts. So for photoelectrons to be emitted from the metal surface, the energy of the incident photons must be greater than the work function, and if this condition is satisfied, then the maximum kinetic energy that the liberated photoelectrons have is given by Equation 2:

$$E_{kmax} = h\nu - |e|\phi \quad (2)$$

where e is the charge on an electron. However, on its own, a single metal surface would quickly become positively charged and would cease to emit photoelectrons. Therefore, by connecting two surfaces together in a circuit; one being an emitter with a lower work function and the other a collector with a higher work function, the current can continue to flow and it can be measured. Figure 1 shows that there is a built-in potential ($V_B = \phi_C - \phi_E$) between the two surfaces, so if a voltage is applied to the circuit, the emitted photoelectrons will need sufficient energy to overcome both the applied voltage (V_{app}) and the built-in potential (V_B) to generate a measurable current. So mathematically, this condition is written as:

$$E_k \geq |e|V \quad (3)$$

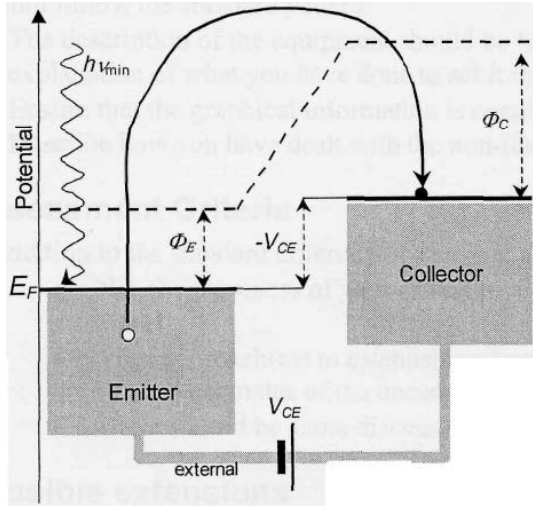


Figure 1: Photocell energy level diagram (with external circuit). This uses the convention of a negative V_{CE} , and E_F is the Fermi energy of each surface.

Thus setting the applied voltage high enough to the cut-off voltage (V_{CE}) means that no current is detected, and the following relation is obtained (see appendix for full derivation):

$$V_{CE} = \frac{h}{|e|} \cdot \nu - \phi_C \quad (4)$$

As the equation suggests, plotting a graph of cut-off voltages for a variety of specific photon frequencies will yield a gradient equal to $h/|e|$.

III. METHODS

The LD Didactic high pressure mercury lamp was the monochromatic light source used, and although no information on the pressure of the mercury lamp could be found¹, it was thought that the lamp should be between 50-100 atm, after comparing it with mercury's characteristic spectrum at these pressures. Five different narrow bandpass spectral filters, with corresponding wavelengths, were used and their data is shown in Table 1 below.

Table 1: Spectral Filter Wavelengths and Information

Colour	Wavelength/nm	Comments
Red*	691.4 ± 2.0	Particularly weak line
Yellow	578.0 ± 2.0	Used to align setup
Green	546.1 ± 2.0	Relatively high intensity
Blue	436.0 ± 2.0	Relatively low intensity
Violet	405.7 ± 2.0	Most energetic photons

¹There was no information of the pressure on the lamp datasheet or on the lamp itself that could be determined.

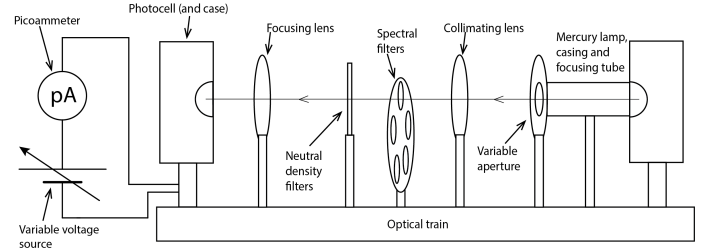


Figure 2: Schematic of experimental setup. The purpose of the neutral density filters were to test that the stopping potential does not depend on intensity.

The target was a Leybold[®] photocell, which contained a potassium/silver oxide-coated cathode ($\phi_E \approx 2.3\text{eV}$) [2] and a platinum-rhodium anode ($\phi_C \approx 6.35\text{eV}$) [2] separated by a vacuum. Suitable precautions were taken to shield the setup from ambient light, prevent overheating, and to minimise anode illumination. As such, an ambient light reading was taken and shown to produce a photocurrent of $0.00005 \pm 0.00003\text{nA}$, which was found to be insignificant to the results, due to other sources of uncertainty.

IV. DATA & RESULTS

Before the measurements and calculations of Planck's constant could commence, the verification of intensity independence was investigated by utilising two methods: varying the size of the aperture window, and also placing neutral density filters in the path of the mercury lamp source to change the intensity.

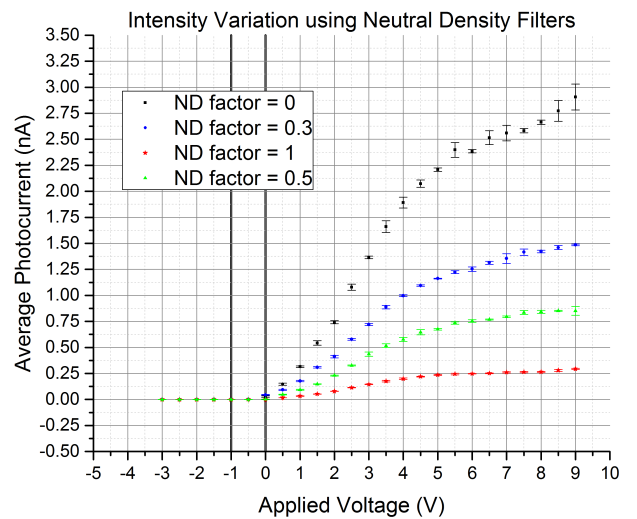


Figure 3: Graph showing average photocurrent for varying intensities. Notice how the cut-off voltage does not deviate from the section marked by the black vertical lines.

Voltage/V	Photocurrent/nA					Average/nA	Std. Dev./nA
	Set 1	Set 2	Set 3	Set 4	Set 5		
-0.25	0.05788	0.05967	0.05873	0.05832	0.05772	0.05846	7.81108E-4
-0.3	0.03467	0.03557	0.0348	0.03623	0.03563	0.03538	6.44515E-4
-0.35	0.02012	0.01963	0.01938	0.02003	0.01943	0.01972	3.40544E-4
-0.4	0.01047	0.01111	0.01051	0.01052	0.01102	0.01073	3.11657E-4
-0.45	0.00489	0.00492	0.00475	0.00509	0.00501	0.00493	1.2853E-4
-0.5	0.00199	0.002	0.00193	0.00205	0.00192	0.00198	5.35724E-5
-0.55	5.3E-4	6.4E-4	4.2E-4	6E-4	4.5E-4	5.28E-4	9.41807E-5
-0.6	-2.1E-4	2E-5	-1.8E-4	1E-5	-5E-5	-8.2E-5	1.07098E-4
-0.65	-4E-4	-4.4E-4	-4.6E-4	-4.3E-4	-3.4E-4	-4.14E-4	4.66905E-5
-0.7	-3.9E-4	-5.9E-4	-4.4E-4	-3.7E-4	-4.3E-4	-4.44E-4	8.6487E-5
-0.75	-4.8E-4	-5.5E-4	-5.6E-4	-5.8E-4	-5.4E-4	-5.42E-4	3.76829E-5
-0.8	-6.7E-4	-6.2E-4	-4.9E-4	-6.8E-4	-5.7E-4	-6.06E-4	7.82943E-5
-0.85	-6.6E-4	-6E-4	-6.8E-4	-6.2E-4	-6.2E-4	-6.36E-4	3.28634E-5
-0.9	-5.7E-4	-6.4E-4	-6.9E-4	-5E-4	-6.3E-4	-6.06E-4	7.30068E-5
-0.95	-6E-4	-5.2E-4	-5E-4	-6.4E-4	-6.7E-4	-5.86E-4	7.4027E-5
-1	-5.4E-4	-5.6E-4	-7.1E-4	-7.1E-4	-5.4E-4	-6.12E-4	8.98332E-5
-1.05	-7.1E-4	-5.4E-4	-6.1E-4	-5.9E-4	-7E-4	-6.3E-4	7.31437E-5
-1.1	-5E-4	-7E-4	-5.6E-4	-5.3E-4	-6.3E-4	-5.84E-4	8.08084E-5
-1.15	-5.3E-4	-5.5E-4	-6.6E-4	-5.8E-4	-7.5E-4	-6.14E-4	9.07193E-5
-1.2	-5.6E-4	-5.6E-4	-6.6E-4	-6.2E-4	-6.1E-4	-6.02E-4	4.26615E-5
-1.25	-8.2E-4	-5.2E-4	-5.5E-4	-6.1E-4	-6.5E-4	-6.3E-4	1.17686E-4

Table 2: Raw data table for green (546nm) wavelength light with basic statistical data is provided on the right.

Figure 3 shows the results of the latter of these two methods for yellow light (578nm) and since the uncertainty in varying the aperture size systematically was very large, these results are the more accurate ones (alternative method graph given in the appendix). Both of these techniques indicate that the value of the stopping voltage does not change with intensity, so this shows that the classical model of the photon is incorrect. It has also been shown that the quantum model is correct in that the cut-off voltage, and thus the energy of the photons, varies with frequency. Figure 4 presents this clearly, showing the cut-off voltage that has been recorded as the intersection with the line at $y = 0$ for different spectral filters.

After this was completed, the cut-off voltage was examined and Table 2 below shows an example of the raw data that was taken, as well as the statistical analysis on the uncertainties that were undertaken. Observing Figures 3 and 4, there are several points of interest to note. Firstly a back current was detected for all of the wavelengths that were investigated when voltages beyond V_{CE} were used. A back current in this situation is caused by photoelectrons liberated from the anode by scattered light, but instead of being emitted from the platinum itself, it is in fact due to

impurities of potassium that have been vapourised and deposited onto the anode surface.

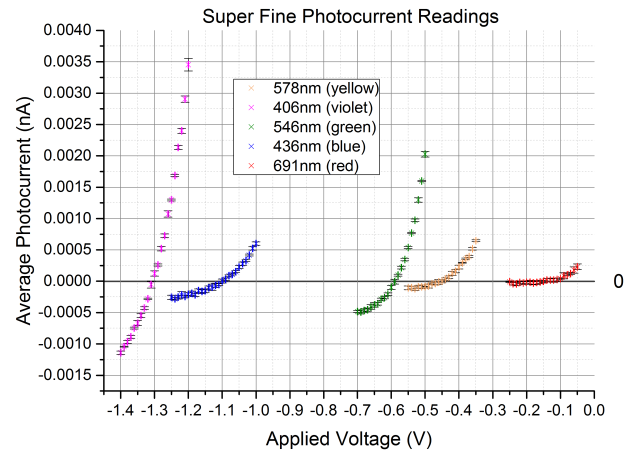


Figure 4: Graph showing the various cut-off voltages for each frequency investigated. Also notice the non-linear behaviour when close to the stopping voltage.

Another feature of Figure 3 is the flattening of the characteristic curve for very high voltages, due to electron saturation. This shows that the number of photo-

electrons liberated has reached a maximum number irrespective of both the increasing number of photons introduced to the system and also the applied voltage. Finally, the non-ohmic behaviour of the photocell is another detail that should not be neglected. Theoretically, the photocell should behave as a diode, with an instantaneous, sudden change at the cut-off voltage. However it is observed that the current rises relatively slowly until it begins to take on the familiar linear form. This can be explained by two ideas: firstly there are heat losses within the circuit that are proportional to I^2 , and also the density of electron states with energy approximately equal to the work function is very small at V_{CE} , but increases with the applied voltage.

i. Zero-Current Crossings

This was the first method of directly determining the cut-off voltage, and it involved determining the x-intercept of the detected photocurrent. To ensure that our readings were precise enough for this to be an acceptable method, we took extra-fine readings that examined the 0.20nA range around the change in photocurrent sign. It was also found that higher intensities were more favourable for this method, since this gives a steeper profile and a more definitive crossing point. Figure 5 shows an example of this finer plot, and Figure 6 shows the plot obtained when values for the cut-off voltage were calculated and plotted for this method of determination.

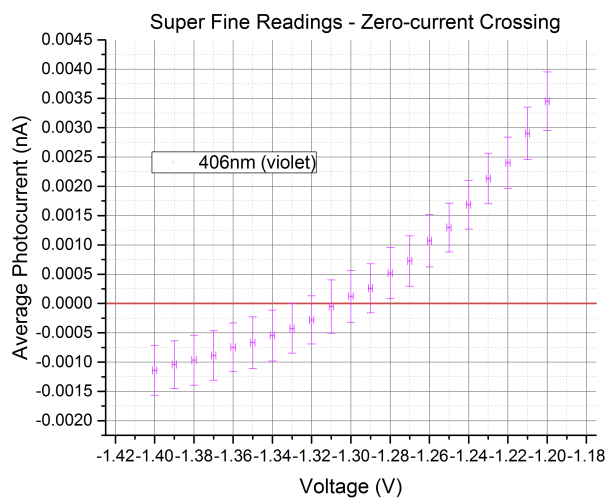


Figure 5: Zero-current crossing plot for violet (406nm) light. As the graph shows, it is an uncertain method of determining the cut-off voltage.

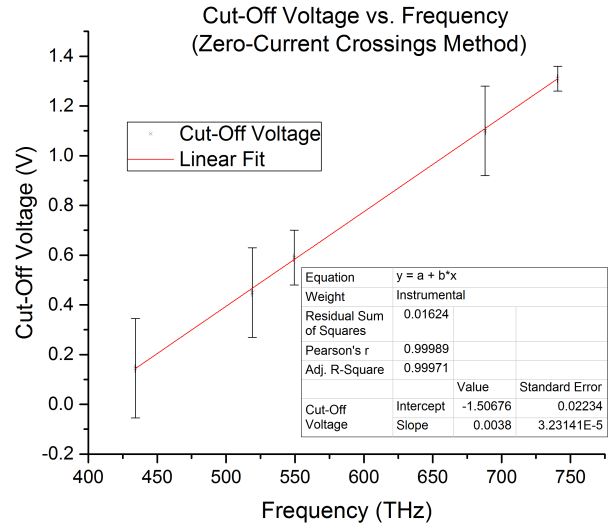


Figure 6: Linear plot of stopping potential against frequency, with data taken using the zero-current crossing point method.

This method had a very good statistical fit, with an R^2 value that was extremely close to 1, indicating a suitable goodness of fit to consider this method. After using error propagation, this method yielded a value of $(6.08 \pm 0.52) \times 10^{-34} \text{ Js}$.

ii. Shockley Diode Equation

In this method, the behaviour of the photocell is approximated to that of a function similar to Shockley's Diode equation, given in Equation 5 below:

$$I(V) = A(e^{B(V-C)} - 1) \quad (5)$$

where A is the 'dark' residual current, B is proportional to the intensity and C is the stopping voltage. This approximation is justified since the photocell ideally acts like a diode when there is a difference between the work functions, meaning that in this model, electrons should only be allowed to flow one way from the cathode to the anode across the vacuum. The fitting itself was done in OriginLab inputting the equation manually and by making some rough estimations for each constant: $A(= 10)$, $B(= 7)$ and $C(= -1)$ and then free-fitting the equation onto the finer results. Figure 7 shows an example of the fitting on fine readings, and Figure 8 shows how the cut-off voltage varies with frequency.

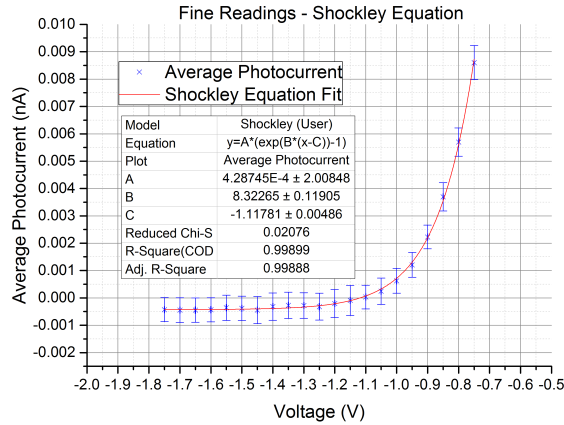


Figure 7: Shockley equation plot and fit for blue (436nm) light. As the graph shows, it is an uncertain method of determining the cut-off voltage.

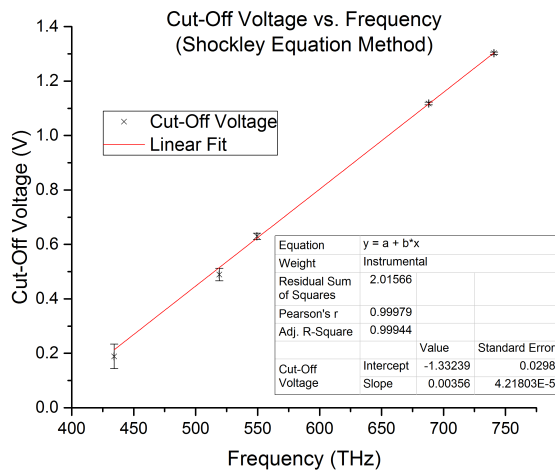


Figure 8: Linear plot of stopping potential against frequency, with data taken using the Shockley Diode equation method.

Overall this method produces a very good fit (apart from at the longest wavelengths) and a low uncertainty value, and as such it yielded a value of $(5.70 \pm 0.07) \times 10^{-34} \text{ J s}$ after error analysis.

iii. Linear Approximation

Since there is approximately asymptotic behaviour for both high and low voltages of the photocell profile, a linear approximation can be made to determine the stopping potential difference. Both sections of the curve were fitted with separate linear regressions and afterwards were extrapolated to determine their intersection. This coordinate is denoted by (V_{CE}, I_0) , where

V_{CE} is an estimate for the stopping voltage and I_0 the base current. For high voltages, the greatest three voltage points were chosen for the linear approximation, by requirement of goodness of fit, whereas for the low voltages the requirement that was set was for the linear approximation to have a gradient between 0 and 1×10^{-4} , as this was a suitable approximation to when the gradient was non-zero. This method yielded a value of $(6.72 \pm 1.64) \times 10^{-34} \text{ J s}$, which was very close to the true value of Planck's constant.

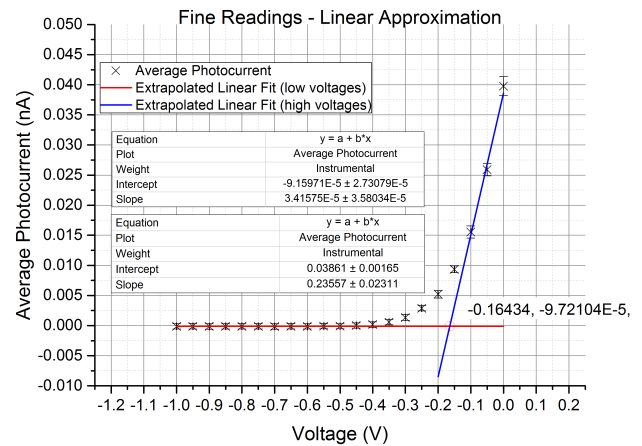


Figure 9: Zero-current crossing plot for yellow (578nm) light. As the graph shows, it is an uncertain method of determining the cut-off voltage.

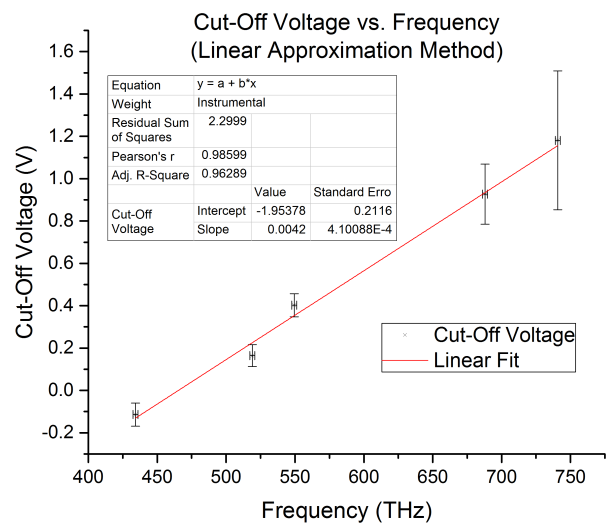


Figure 10: Linear plot of stopping potential against frequency, with data taken using the linear approximation intersection method.

V. UNCERTAINTIES & DISCUSSION

So the overall result of the three analysis methods gave an average h value of $6.17 \times 10^{-34} \text{Js}$ with a total error of $6.82 \times 10^{-34} \text{Js}$. The sources of uncertainty shall now be explored and error calculations will be explained.

According to Equation 4, the y-intercept of the plots of voltage against frequency should correspond to the work function of the anode, made of platinum ($\phi_C \approx 6.35 \text{eV}$). However, this is still not well represented by the data and one of the main reasons for this is due to the external quantum efficiency of the photocell.

$$EQE = \frac{\text{photocurrent}/|e|}{\text{detected power}/h\nu} \quad (6)$$

This was calculated, using a power meter and Equation 6, to be $0.00886 \pm 0.00204\%$, and since this value is very much less than 100%, this means for a certain number of photons there will be much fewer liberated photoelectrons than expected. Hence the measured photocurrent will be lower and this will affect the y-intercept of the graph, but not the gradient of the plot of V_{CE} vs ν . If the main objective was to accurately calculate the work function of the collector, certain aspects of the experiment would need to be transformed, such as baking the photocell to remove deposits from the anode ring and taking precautions ensuring that deposits do not reappear, use purer metals in the photocell instead of alloys, and also take a larger range of readings.

In this investigation, only the uncertainties in the gradients of the plots are of real interest, and these can be split up into two types:

- **Systematic error (σ_s)** - the propagation of errors from all three different methods used to evaluate the cut-off voltage
- **Random error (σ_r)** - the *true* standard deviation in the raw data that was taken (calculated with the inclusion of Bessel's correction)

Any linear regression calculated from datasets will give an uncertainty in its gradient and its y-intercept. So when finding the intersection of two of these extrapolated lines, given by $y = m_1x + c_1$ and $y = m_2x + c_2$, requires the correct error propagation formula. So the error in the x-coordinate of the intersection point is given below in Equation 7:

$$\sigma_x^2 = \left(\frac{1}{m_1 - m_2} \right)^2 \sigma_{c_1}^2 + \left(\frac{1}{m_1 - m_2} \right)^2 \sigma_{c_2}^2 + \left(\frac{c_2 - c_1}{(m_1 - m_2)^2} \right)^2 \sigma_{m_1}^2 + \left(\frac{c_2 - c_1}{(m_1 - m_2)^2} \right)^2 \sigma_{m_2}^2 \quad (7)$$

Also, when calculating the uncertainties in the individual values of h from the gradients, the propagation of errors shows that:

$$\sigma_h^2 = |e| \sigma_{\text{gradient}}^2 \quad (8)$$

which is very convenient. Now that all the uncertainties have been individually accounted for, the actual value of h can be determined by taking the average value (\bar{h}) and suitably propagating the associated error for each method ($\bar{\sigma}_h$):

$$\sigma_{\text{total}}^2 = \sigma_r^2 + \sigma_s^2 \quad (9)$$

where in this case:

$$\sigma_r^2 = \frac{1}{9} \sum_i \sigma_{h_i}^2 = 3.29 \times 10^{-69} \text{J}^2 \text{s}^2 \quad (10)$$

$$\sigma_s^2 = \frac{1}{3} \sum_i \langle h_i^2 \rangle - \langle h_i \rangle^2 = 1.36 \times 10^{-69} \text{J}^2 \text{s}^2 \quad (11)$$

VI. CONCLUSIONS & FUTURE DEVELOPMENT

In conclusion, it has been shown that in this context light behave as a particle in its interaction with matter, and as such follows the quantum description of photons. Through this investigation, the energy of said photons has been demonstrated to be independent of intensity and linearly dependent on wavelength, and the experiment has determined the constant of proportionality with some degree of accuracy. The actual value of Planck's constant fell outside of the error bars, which is unsatisfactory, but the associated error is very good (roughly 10% of the calculated average value of h).

In terms of improving the errors themselves, this can be split again into the random and systematic errors of the investigation. Reducing the random errors can be accomplished by using more *independent* trials, as well as additional sets of repeat readings. This is because in allowing the picoammeter and variable voltage supply to be switched off and not used between each trial, or alternatively one could wait for a longer period of time between sets of readings, a more accurate variance may be observed in the measurements. For the systematic error, simply taking more data points and extending our observations further into the high and low voltage ends means that there is much more information to reduce the systematic error. Furthermore, a brighter photon source, such as a laser, would offer a much greater resolution for the current vs. voltage plots and also produce a better estimate for the cut-off voltage.

There are many areas for further exploration within this experiment as well, and a major one is changing other system variables, such as the intensity and the cathode, or anode, work function. Investigating their effects on the system may provide further evidence on the particle nature of light, as well as an independent source of results to confirm this investigation. Alternatively as described earlier, the experiment itself could be adjusted to measure the value of the collector work function, and consequently the emitter work function, thus providing a better picture on the inner workings of the photocell itself.

Word Count (checked in Word): 2913

REFERENCES

- [Hertz, 1887] Hertz, H. (1887). "Ueber den Einfluss des ultravioletten Lichtes auf die electrische Entladung" [On an effect of ultra-violet light upon the electrical discharge]. *Annalen der Physik*. 267 (8): S. 983-1000
- [Einstein, 1905] Einstein, Albert (1905). "Über einen die Erzeugung und Verwandlung des Lichtes betreffenden heuristischen Gesichtspunkt" [On a heuristic viewpoint concerning the production and transformation of light]. *Annalen der Physik*. 17 (6): 132-148
- [1] The NIST Reference for Constants, Units and Uncertainties (2014). Obtained at <http://physics.nist.gov/cgi-bin/cuu/Value?h>
- [2] Obtained from <http://hyperphysics.phy-astr.gsu.edu/hbase/tables/photoelec.html>

VII. APPENDICES

i. Derivation of Equation 4

This shows the individual steps from the maximum kinetic energy of the photoelectrons to the main equation of this investigation. So starting from Equation 2:

$$E_{kmax} = h\nu - |e|\phi_E \quad (12)$$

and we also know that:

$$V_B = (\phi_C - \phi_E) \text{ \& } V_{CE} = V_{app} + V_B \quad (13)$$

So when we are applying the cut-off voltage exactly, the following equality (from Equation 3) applies:

$$E_k = |e|V_{CE} \quad (14)$$

Substituting (13) into (14) gives:

$$h\nu - |e|\phi_E = |e|(V_{app} + V_B) \quad (15)$$

and rearranging:

$$h\nu - |e|\phi_E = |e|(V_{app} + \phi_C - \phi_E) \quad (16)$$

$$h\nu = |e|V_{app} + \phi_C \quad (17)$$

and so we get to Equation 4:

$$V_{app} = \frac{h}{|e|} \cdot \nu - \phi_C \quad (18)$$

So this means that applying a voltage $V_{app} = V_{CE}$ will result in no significant photocurrent being detected in a setup described in Figure 1.

ii. Alternative Method for Verifying Intensity Independence

Below is the graph with which the method of varying the aperture window size was used.

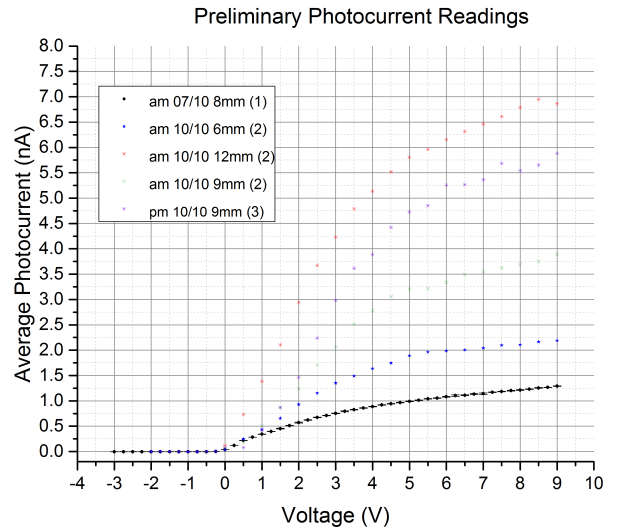


Figure 11: Graph showing average photocurrent for varying intensities. Notice how the cut-off voltage does not deviate much from the same area.